



Published in final edited form as:

*Eur J Pharmacol.* 2020 October 15; 885: 173419. doi:10.1016/j.ejphar.2020.173419.

## Rosmarinic acid-induced apoptosis and cell cycle arrest in triple-negative breast cancer cells

Samia S. Messeha, Najla O. Zarmouh, Abrar Asiri, Karam F.A. Soliman\*

Division of Pharmaceutical Sciences, College of Pharmacy & Pharmaceutical Sciences, Florida A&M University, 1415 ML King Blvd, Room G 134 H New Pharmacy Building, Tallahassee, FL, 32307, United States

### Abstract

Rosmarinic acid (RA) is a polyphenolic compound with various pharmacological properties, including, anti-inflammatory, immunomodulatory, and neuroprotective, as well as having antioxidant and anticancer activities. This study evaluated the effects and mechanisms of RA in two racially different triple-negative breast cancer (TNBC) cell lines. Results obtained show that RA significantly caused cytotoxic and antiproliferative effects in both cell lines in a dose- and time-dependent manner. Remarkably, RA induced cell cycle arrest-related apoptosis and altered the expression of many apoptosis-involved genes differently. In MDA-MB-231 cells, RA arrested the cells in the G<sub>0</sub>/G<sub>1</sub> phase. In contrast, the data suggest that RA causes S-phase arrest in MDA-MB-468 cells, leading to a 2-fold increase in the apoptotic effect compared to MDA-MB-231 cells. Further, in MDA-MB-231 cells, RA significantly upregulated the mRNA expression of three genes: harakiri (*HRK*), tumor necrosis factor receptor superfamily 25 (*TNFRSF25*), and BCL-2 interacting protein 3 (*BNIP3*). In contrast, in the MDA-MB-468 cell line, the compound induced a significant transcription activation in three genes, including *TNF*, growth arrest and DNA damage-inducible 45 alpha (*GADD45A*), and *BNIP3*. Furthermore, RA repressed the expression of TNF receptor superfamily 11B (*TNFRSF11B*) in MDA-MB-231 cells in comparison to the ligand TNF

This is an open access article under the CC BY-NC-ND license (<http://creativecommons.org/licenses/by-nc-nd/4.0/>).

\*Corresponding author. karam.soliman@fam.u.edu (K.F.A. Soliman).

#### Authors' contributions

Conceptualization, SSM and KFAS; methodology, SSM and AA; software, SSM; validation, SSM, KFAS, and AA; formal analysis, SSM and AA; investigation, SSM, KFAS, and AA; resources, KFAS; data curation, SSM and KFAS; writing original draft, SSM; writing – review & editing: SSM, NZ, AA, and KFAS; visualization, SSM; supervision, SSM and KFAS; project administration, SSM and KFAS; funding acquisition, KFAS. All authors read and approved the manuscript and accept to be responsible for all aspects of the research in ensuring that the accuracy or integrity of any part of the work is properly considered.

#### Declaration of competing interest

The authors state that they have no competing interest.

#### Authors agreement

All authors declare that there is no conflict of interest regarding the work performed in this manuscript. We further declare that the work described has not been published previously (except in the form of an abstract), that it is not under consideration for publication elsewhere, that its publication is approved by all authors and tacitly or explicitly by the responsible authorities where the work was carried out, and that, if accepted, it will not be published elsewhere in the same form, in English or in any other language, including electronically without the written consent of the copyright-holder.

#### Ethics approval and consent to participate

Not applicable.

#### Patient consent for publication

Not applicable.

#### Availability of data and materials

All data generated or analyzed during this study are included in this published article.

superfamily member 10 (*TNFSF10*) and baculoviral IAP repeat-containing 5 (*BIRC5*) in MDA-MB-468 cells. In conclusion, the data suggest that the polyphenol RA may have a potential role in TNBC therapies, particularly in MDA-MB-468 cells.

## Keywords

Rosmarinic; Triple-negative breast cancer; Apoptosis; Cell cycle; Gene expression

---

## 1. Introduction

Molecular-targeted therapies require an understanding of the mechanisms linking cancer, apoptosis, and drug resistance (Fulda, 2011; Johnstone et al., 2002). One attractive strategy for cancer therapy is to trigger cancer cell death pathways through the development of apoptotic inducer drugs in concert with other anticancer medications (Jan and Chaudhry, 2019). Mounting evidence shows that cell cycle arrests and apoptosis can sensitize cancer cells to radiotherapy or chemotherapy (Ryu et al., 2018; Zhang et al., 2018).

Apoptosis is a unique cell death mechanism that regulates development and maintains homeostasis of the cell through controlled signaling pathways. Apoptosis as a genetically programmed event, however, is frequently altered and/or impaired in cancer cells, leading to malignancy, metastasis, and chemotherapy resistance (Fulda, 2009; Plati et al., 2008). Cancer cells often resist apoptosis by upregulating anti-apoptotic proteins or attenuating the expression of proapoptotic proteins (Messeha et al., 2019). Additionally, in aggressive metastatic phenotypes, overexpression of Bcl-2 protein may increase the ability of the cancer cell to resist apoptotic death by interrupting the intrinsic apoptotic signaling pathway. Likewise, in multiple cancer cells, the upregulation of the inhibitor of apoptosis (IAP) members promotes chemoresistance (Fulda, 2008). Therapeutics that target the IAP pathway might be exploited as a molecular target for apoptosis-inducing approaches to cancer treatment (LaCasse et al., 2008).

Breast cancer comprises a diverse set of malignancies with a substantial global burden. Triple-negative breast cancer (TNBC) is a very aggressive and metastatic subtype (Dai et al., 2019). In particular, many TNBC cases have a worse outcome after chemotherapy (Anders and Carey, 2009). TNBC treatment opportunities are limited because of the lack of the three specific receptors: estrogen (ER), progesterone (PR), and human epidermal growth factor (Her2/neu) (Sadighi et al., 2017) (Hudis and Gianni, 2011).

Rosmarinic acid (RA) is one of the potent polyphenolic compounds in rosemary (*Rosmarinus officinalis*) extract. In cancer research, the natural compound RA has been recognized as a potent agent in various cancer cell lines, including breast cancer (Yesil-Celiktas et al., 2010). RA also has been found to have an apoptotic effect in different types of cancer, including breast (Li et al., 2018). Furthermore, RA has been observed to augment the apoptotic effect of chemotherapeutic, adriamycin (Huang et al., 2018).

Thus, this study was undertaken to explore the anticancer mechanisms of the polyphenolic compound RA on two human TNBC cell lines, MDA-MB-231 and MDA-MB-468. We

assessed the potential effects of RA on cell viability, proliferation, cell cycle arrest, and apoptosis. We hypothesized that the apoptotic effects of RA might be due to its ability to alter the expression of different apoptosis-related genes that mediate these events.

## 2. Materials and methods

### 2.1. Materials and reagents

RA (purity 98%) and Alamar Blue® (a solution of resazurin fluorescence dye) were purchased from Sigma-Aldrich (St. Louis, MO, USA). Trypsin-EDTA solution, penicillin/streptomycin, and Dulbecco's phosphate-buffered saline (DPBS) were obtained from the American Type Culture Collection (ATCC; Manassas, VA, USA). An Annexin V-FITC Apoptosis Detection Kit Plus (cat. no. 68FT-Ann VP-S) was purchased from RayBiotech (Norcross, GA, USA). Propidium Iodide Flow Cytometry Kit (cat. No. ab139418) was purchased from Abcam (Cambridge, MA, USA). A DNA-free™ kit (cat. no. AM1907) was purchased from Life Technologies, Inc. (Thermo Fisher Scientific, Inc., Waltham, MA, USA). An iScript™ cDNA Synthesis kit (cat. no. 170-8890), SsoAdvanced™ Universal SYBR® Green Supermix, and the Human Apoptosis PCR array (SAB Target List) H96 were purchased from Bio-Rad Laboratories (Hercules, CA, USA). Dulbecco's modified Eagle's medium (DMEM) and heat-inactivated fetal bovine serum (FBS) were purchased from VWR International (Radnor, PA, USA). Cell culture flasks were purchased from Santa Cruz Biotechnology, Inc. (Dallas, TX, USA). Cell culture plates were purchased from Thermo USA Scientific (Ocala, FL, USA).

### 2.2. Cell culture

Two TNBC cell models, MDA-MB-231 (ATCC® HTB-26™) and MDA-MB-468 (ATCC® HTB-132™) were purchased from ATCC. Both cell lines were grown as monolayers in 75-ml tissue culture (TC) flasks at 37 °C in a humidified 5% CO<sub>2</sub> incubator and subculture as required with trypsin/EDTA (0.25%). The complete growth DMEM contained 4 mM L-glutamine and was supplemented with 10% heat-inactivated FBS (v/v) and 1% penicillin/streptomycin salt solution (100 U/ml and 0.1 mg/ml, respectively). DMEM supplemented with 2.5% heat-inactivated FBS was used as the experimental media (Sato et al., 1993).

### 2.3. Cell viability assay

The cytotoxicity of RA on BC cells was determined in MDA-MB-231 and MDA-MB-468 cells using Alamar Blue® (Messeha et al., 2019). Cells were plated at a density of  $2 \times 10^4$  cells/well in 96-well plates and incubated overnight at 37 °C. RA was solubilized in cell culture water, and both cell lines were treated for 48 h with the compound at concentration ranges from 0 to 500 µM. Wells treated in the same manner but without cells were used as blanks. The experiments were performed in triplicates. After 48 h, 20 µl Alamar Blue® was added to each well and incubated for 4h at 37 °C. The reduced resazurin dye was measured at an excitation/emission wavelength of 530/590 nm using a Synergy HTX Multi-Mode microplate reader (BioTek Instruments, Inc., Winooski, VT, USA).

#### 2.4. Cell proliferation assay

Alamar Blue® assay was used to determine the effect of RA on cell proliferation for MDA-MB-231 and MDA-MB-468 TNBC cells. Briefly, cells were seeded in 96-well plates ( $1 \times 10^4$  cells/well) and incubated overnight at 37 °C. Both MDA-MB-231 and MDA-MB-468 cell lines were treated for 72 and 96 h with RA at the same concentrations ranging from the viability assay (0–500  $\mu$ M) in a final volume of 200  $\mu$ l/well (Citalingam et al., 2015). Equivalent wells without cells were used as a blank. At the end of each exposure period, 20  $\mu$ l of Alamar Blue® was added to each well, incubated for 4 h at 37 °C and the plates were read at an excitation/emission wavelength of 530/590 nm using a Synergy HTX Multi-Mode microplate reader (BioTek Instruments, Inc., Winooski, VT, USA).

#### 2.5. Cell cycle analysis

The effect of RA on DNA content and cell cycle distribution was determined for both MDA-MB-231 and MDA-MB-468 cell line following previously described protocols (Cao et al., 2018; Kuo et al., 2006). Briefly, cells were seeded overnight at  $1.5 \times 10^6$  cells/T25 cell culture flasks and then treated with RA at 125 and 250  $\mu$ M concentration levels in a final volume of 6 mL/flask of experimental media. After 48 h, both floating and attached cells were collected, pelleted, washed with PBS, and fixed in cold 70% ethanol. The cells were again pelleted, washed in DPBS, and gently resuspended in 200  $\mu$ l 1X propidium Iodide (PI) + RNase staining solution followed by incubation at 37 °C in the dark for 30 min. For each sample,  $1 \times 10^4$  cells were examined for cell cycle distribution using a FACSCalibur flow cytometer (BD Biosciences, San Jose, CA, USA). Data acquisition and data analysis were performed using CellQuest software (BD Biosciences, San Jose, CA, USA).

#### 2.6. Apoptosis assay

The apoptotic effect of RA was determined in MDA-MB-231 and MDA-MB-468 cells using the previously described protocol (Messeha et al., 2019). Briefly, in separate experiments, MDA-MB-231 and MDA-MB-468 cells were plated in 6-well plates ( $5 \times 10^5$  cells/well) and incubated overnight at 37 °C. In experiments designed to induce apoptosis, cells were similarly treated with RA at concentrations ranging from 0 to 400  $\mu$ M in a final volume of 3 ml/well of experimental media, and control cells were exposed to only experimental media. After 48 h exposure period, treated and control cells from each well were harvested, pelleted, and washed in DPBS. Subsequently, the cell pellets were suspended in 500  $\mu$ l of 1X Annexin V binding buffer and labeled with 5  $\mu$ l of Annexin V-FITC and PI. The apoptotic effect was measured within 5–10 min using a FACSCalibur flow cytometer (BD Biosciences, San Jose, CA, USA). For each sample,  $1 \times 10^4$  cells were examined, and CellQuest software (BD Biosciences, San Jose, CA, USA) was used for acquisition and data analysis.

#### 2.7. Quantitative reverse transcription-polymerase chain reaction (qRT-PCR) apoptosis array

Both MDA-MB-231 and MDA-MB-468 cells were treated with 350  $\mu$ M of RA. The chosen concentration is close to the  $IC_{50}$  values in the viability study and did not show a significant necrotic effect in the apoptosis assay (Ramachandran et al., 2005) (Rahman et al., 2006)

(Teoh et al., 2019). Briefly, for each cell line, two T-75 flasks of  $6 \times 10^6$  cells representing the control and treated cells were incubated overnight at 37 °C, followed by a 48-h treatment period. The cells from each flask were harvested without trypsinization, pelleted, and washed twice with DPBS. The total RNA was extracted from treated cells with 1 ml of TRIzol reagent as recommended by the manufacturer. For each phase separation, 0.2 ml of chloroform was added to each sample, vortexed, incubated at room temperature (RT) for 2–3 min and centrifuged for 15 min at  $10,000 \times g$  at 2–8 °C. The aqueous phase was collected in fresh centrifuge tubes and mixed with 0.5 ml of isopropyl alcohol to pellet the RNA. The RNA pellets were then washed with 75% ethanol and reconstituted in nuclease-free water (~30–50  $\mu$ l) and placed in an –80 °C freezer for later use. RNA quantity and purity were measured in each sample using a NanoDrop spectrophotometer (NanoDrop Technologies; Thermo Fisher Scientific, Inc.). Lastly, cDNA for the control and treated cells was synthesized using the iScript™ cDNA Synthesis kit; and the obtained cDNA was kept in a –80 °C freezer. Each well of the 96-well human apoptosis array was loaded with 10  $\mu$ l each of the reconstituted cDNA (2.3 ng) and SsoAdvanced™ Universal SYBR® Green Supermix, and the plate placed for 5 min in a shaker and centrifuged at  $1000 \times g$  for 1 min. The fluorescent quantitative PCR run was established using a Bio-Rad CFX96 Real-Time System (Bio-Rad Laboratories) with 39 thermo-cycling of denaturation (Yamamoto et al., 2009) as follows: 30-s activation at 95 °C, 10-s denaturation at 95 °C; 20-s annealing at 60 °C; and 31-s extension at 65 °C. All RT-PCR results were confirmed by three independent experiments for each cell line. Gene expression was analyzed using the CFX 3.1 Manager software (Bio-Rad Laboratories) and verified with Student's t-test.

## 2.8. Statistical analysis

Data from this study were analyzed using GraphPad Prism 6.2 software (GraphPad Software, Inc., San Diego, CA, USA). All data points present the average of at least two independent experiments and are expressed as the mean  $\pm$  S.E.M. The  $IC_{50}$ s values were calculated by nonlinear regression model of log (inhibitor) vs. normalized response-variable slope on the software with the  $R^2$  best fit and the lowest 95% confidence interval. The average of  $IC_{50} \pm$  S.E.M. was calculated on an Excel sheet. The significance of the difference was determined using one-way or two-way analysis of variance (ANOVA) as indicated in the legends followed by Bonferroni's multiple comparison test. Gene expression data were analyzed using CFX 3.1 Manager software (Bio-Rad Laboratories). Unpaired Student t-test was used for comparing two data sets. Generally, a difference was considered significant at  $*P < 0.05$  (as indicated in the figures and legends).

## 3. Results

### 3.1. Rosmarinic acid decrease of the cell viability of triple-negative breast cancer cells

To evaluate the potential anticancer effect of RA in TNBC, we assessed cell viability in two TNBC cell lines, MDA-MB-231 and MDA-MB-468, at concentration ranges of 0–500  $\mu$ M of the compound. The dose-response of the two cell lines to RA was similar, as indicated in Fig. 1A and B ( $IC_{50} = 321.75 \pm 9.75$  for MDA-MB-231 cells and  $340.45 \pm 7.57$   $\mu$ M for MDA-MB-468 cells). An apparent dose-dependent decrease in cell viability was detected in both cell lines at concentration levels 125–500  $\mu$ M ( $P < 0.0001$ ). In contrast to MDA-

MB-231 cells, a small reduction in cell viability was found in MDA-MB-468 cells at lower concentrations of RA (15.62–62.5  $\mu\text{M}$ ,  $P < 0.05$ – $P < 0.01$ ). These changes imply a higher sensitivity of this cell line to RA.

### 3.2. Rosmarinic acid inhibition of cell the proliferation of triple-negative breast cancer cells

Antiproliferative assays were performed to evaluate the indirect cytotoxic effect of RA on MDA-MB-231 and MDA-MB-468 TNBC cells, as indicated by the growth-inhibitory potency at more extended exposure periods. Overall, the data obtained indicated a reduction in the proliferation rate in a dose-and time-dependent pattern. In both cell lines, RA significantly inhibited cell proliferation at the 72 and 96 h treatment periods vs. control (Fig. 2A and B;  $P < 0.001$ – $P < 0.0001$ ). Furthermore, the compound induced a highly significant ( $P < 0.0001$ ) antiproliferative effect at 72 vs. 96h exposure period (concentration range 31.25–250  $\mu\text{M}$  in MDA-MB-231 and 15.62–125  $\mu\text{M}$  in MDA-MB-468 cell line) as indicated by the significant reduction in the  $\text{IC}_{50}$  values, in particular for MDA-MB-468 cells. The  $\text{IC}_{50}$  values were reduced from 134.5 to 88.0  $\mu\text{M}$  in MDA-MB-231 cells (Fig. 2A) and from 128 to 64.28  $\mu\text{M}$  in MDA-MB-468 cells (Fig. 2B) at the 72h vs. 96h exposure periods, respectively. On the other side, a non-significant inhibition was noticed at 15.62 as well as 300–500  $\mu\text{M}$  in MDA-MB-231 cells (Figs. 2A) and 250–500  $\mu\text{M}$  in its counterpart MDA-MB-468 cell line (Fig. 2B). Contrary to the viability study data, the response of the MDA-MB-468 cell line to RA antiproliferative effect was slightly higher than MDA-MB-231 cells. These different behaviors of RA against each cell line may indicate underlying different molecular mechanisms for an anticancer effect. In comparison to chemotherapy drugs, our recently published data (Messeha et al., 2019) stated the  $\text{IC}_{50}$  value of cells following 72 h of exposure to doxorubicin as  $1.69 \pm 0.11$  and  $0.23 \pm 0.003$  in MDA-MB-231 and MDA-MB-468 cells, respectively.

### 3.3. Rosmarinic acid-induced cell cycle arrest in triple-negative breast cancer cells

To gain insight into the mechanism underlying the cytotoxic and antiproliferative effects of RA, flow cytometric analysis using PI staining was performed to evaluate the cell cycle distribution in MDA-MB-231 and MDA-MB-468 cell lines after 48h exposure at 125 and 250  $\mu\text{M}$  of RA. The data presented in Fig. 3A indicates that RA treatment at these exposure levels did not severely impact the cell cycle distribution in MDA-MB-231 treated cells. However, a minor but significant ( $\sim 10\%$ ,  $P < 0.0001$ )  $\text{G}_0/\text{G}_1$  phase arrest was observed compared to the control, accompanied by a significant decrease in S-phase cells ( $P < 0.0001$ ). There was also an increase in the number of dead MDA-MB-231 cells (Sub  $\text{G}_1$ ,  $18.56 \pm 0.31$ ), especially at the higher 250  $\mu\text{M}$  RA concentration, as seen to the left of the  $\text{G}_0/\text{G}_1$  peak in (Fig. 3A).

The effect of RA on cell cycle progression was more evident in MDA-MB-468 cells (Fig. 3B). A highly significant 20% increase in S-phase cells ( $P < 0.0001$ ) was found in RA treated cells compare to the untreated control cells ( $45.47 \pm 1.55$  or  $46.75 \pm 0.52$  vs.  $26.50 \pm 0.03$  in control cells) and again demonstrating a differential response to RA in MDA-MB-468 cell as compared with the MDA-MB-231 cell line.

### 3.4. Rosmarinic acid-induced apoptotic effect in triple-negative breast cancer cells

Next, flow cytometer apoptosis analysis, using Annexin V-FITC/PI double staining, was performed to further comprehend the mechanism of growth inhibition in RA-treated TNBC cell lines. After 48h exposure period to RA at concentration ranges 0–400  $\mu$ M, a significant ( $P < 0.05$ – $P < 0.0001$ ) dose-dependent apoptotic effect was observed in both cell lines (Fig. 4A and B). The apoptotic effect was slower in MDA-MB-231 cells compared with its counterpart MDA-MB-468 cell line, which was twice as sensitive to RA. When treated with 400  $\mu$ M of RA, 77.61% of the MDA-MB-468 cells analyzed were in an apoptotic phase, whereas 37.74% of MDA-MB-231 cells exhibited apoptotic effects. A minor component of the necrotic cell (7.44% in MDA-MB-231 cells and 0.32% in MDA-MB-468 cells) were also detected. While RA has similar cytotoxic effects in both cell lines, the apoptosis analysis again demonstrated that the MDA-MB-468 cell line is more sensitive to this agent than are the MDA-MB-231 cells. RA has a more significant antiproliferative effect on these cells. Flow cytometry apoptosis analysis suggests that RA causes MDA-MB-231 cells to be arrested in the  $G_0/G_1$  phase, while the MDA-MB-468 becomes arrested in the S-phase and then undergo apoptosis rather than proceed to  $G_2/M$ .

### 3.5. Rosmarinic acid altered the expression of apoptosis-related genes in triple-negative breast cancer cells

In further analysis, quantitative reverse transcription-PCR (qRT-PCR) for an array of apoptosis genes was performed to determine the molecular effects of RA on MDA-MB-231 and MDA-MB-468 cell lines. The profiled normalized mRNA expression revealed the influence of RA on several apoptosis-related genes. Those significantly upregulated/downregulated genes with  $>2$ -fold change in transcription are presented in Figs. 5–7. In both cell lines, the fold changes in expression and P values are given in Table 1. The data suggest the ability of RA to alter the expression of five genes in MDA-MB-468 cells significantly, and four genes in MDA-MB-231 cells.

The expression of BCL-2 interacting protein 3 (*BNIP3*) was significantly upregulated in both cell lines (Fig. 7A and B), but the *BNIP3* mRNA was upregulated in MDA-MB-468 cells  $\sim 2$ -fold higher than it was for the MDA-MB-231 cells (3.91 ( $P < 0.0087$ ) vs. 2.21 ( $P < 0.0295$ )-fold increase; Table 1). An increase in apoptosis-related gene expression was also found in MDA-MB-231 cells for two more genes (Fig. 7A). Harakiri (*HRK*) was upregulated by 3.38-fold, and TNF receptor superfamily 25 (*TNFRSF25*) had a 3.21-fold increase in its mRNA. Meanwhile, more than 4-fold repression in TNF receptor superfamily 11B (*TNFRSF11B*) gene expression was detected in MDA-MB-231 cells (Table 1).

Considerably more apoptosis-related genes changes were found in RA-treated MDA-MB-468 cells, as compared to MDA-MB-231. Two members of the TNF family of genes were greatly and significantly impacted ( $P < 0.05$ ) (Fig. 7B and Table 1). *TNF* expression was upregulated by 8.50-fold, while the ligand TNF superfamily member 10 (*TNFSF10*) was repressed by higher than 11-fold, as shown in Table 1. Also, a member of the inhibitor of apoptotic proteins (IAPs) family, baculoviral IAP repeat-containing 5 (*BIRC5*) inhibition was highly significant (6.19-fold;  $P < 0.0005$ ). Moreover, growth arrest and DNA damage-

inducible 45 alpha (*GADD45A*) expression were (~5-fold) increased. RA did not show significant alterations in the expression of the different caspases (data not shown).

#### 4. Discussion

Targeting the cell cycle-mediate apoptosis pathway is a rational approach for enhancing tumor sensitivity in coordination with anticancer agents (Katsman et al., 2009). The present study provides an analysis of apoptotic proteins participating in the anticancer effect of the natural polyphenol compound RA. The results suggest two markedly different mechanisms in altering apoptosis-related gene expressions between two racially different TNBC cell lines: MDA-MB-231 and MDA-MB-468.

The study indicated that in the two cell lines, RA differently induced cell cycle arrest and apoptosis. Interestingly, RA arrested the cell cycle of MDA-MB-468 cells early in mitosis and had a more significant apoptotic effect than it did in MDA-MB-231 cells. Further, RA significantly upregulated the mRNA expression of three apoptosis-related genes in the MDA-MB-468 cells, two of which were not affected in MDA-MB-231 cells. Instead, and to a lesser extent, two apoptosis-related genes in MDA-MB-231 cells were upregulated. Also, RA repressed the expression for two genes in MDA-MB-468 cells, while only one apoptosis-related gene was inhibited in the MDA-MB-231 cell line. Initially, the current data indicate that RA shows two distinct molecular mechanisms to inhibit TNBC cell proliferation.

RA showed cytotoxic and antiproliferative effects in both TNBC cell lines, parallel to other reports (Yesil-Celiktas et al., 2010). Similarly, several *in-vitro* studies have shown the ability of RA to inhibit cell proliferation and induce cell cycle arrest and caspase-independent apoptosis in various cancer cells (Jang et al., 2018; Li et al., 2018). Consistently, we found that RA arrested MDA-MB-468 cell cycle progression at the S-phase, induced apoptosis, and decreased proliferation. In contrast, in MDA-MB-231 cells, the compound principally induced G<sub>0</sub>/G<sub>1</sub> cell cycle arrest, having a weaker apoptotic effect as compared with MDA-MB-468 cells. Therefore, we presume that the RA antiproliferative effect in MDA-MB-231 cells does not rely solely on apoptosis.

In this study, RA induced apoptosis by altering the expression of several genes that regulating the extrinsic and intrinsic apoptotic pathways. In the TNBC cells, RA impacted the mRNA expression of *TNF-α* and *TNFSF10* in MDA-MB-468, while it altered *TNFRSF25* and *TNFRSF11B* genes in MDA-MB-231 cells. One reported molecular mechanisms of RA-induced apoptosis involves the mitochondrial apoptotic pathway (Hur et al., 2004).

Thus, the current data adds insight into the potential role of TNF/TNF receptor superfamily in RA-mediated apoptotic effect in human cancer, in agreement with a previous *in vivo* study, (Silva et al., 2014). In MDA-MB-231 cells, RA induced a significant increase in transcription activation of *TNFRSF25* (3.21-fold), while inhibited *TNFRSF11B* by 4.65-fold. These genes were not significantly affected in its counterpart cell line, MDA-MB-468. The gene *TNFRSF25/DR3* is involved in several programmed cell death signaling, including

the nuclear factor  $\kappa$ B (NF- $\kappa$ B), p38 mitogen-activated protein kinase (MAPK), and caspase activation. Compared to healthy tissues, reduced *TNFRSF25* expression is present in the MDA-MB-231 cell line, and this deficit correlates with a poorer prognosis and a significantly shorter survival rate (Ge et al., 2013). On the other hand, the *TNFRSF11B* expression inhibits the extrinsic apoptotic pathway and enhancing cancer cell survival (Silva et al., 2014). Thus, inhibiting the gene expression in RA-treated MDA-MB-231 cells may be a specific target in TNBC therapy.

In contrast, 8.50-fold upregulation of the *TNF/TNF- $\alpha$*  gene expression was noticed in RA-treated MDA-MB-468 cells. The multifunctional *TNF- $\alpha$*  cytokine is the most potent inducer of apoptosis in the TNF superfamily (Rath and Aggarwal, 1999). This finding may explain the higher response of this cell line to the apoptotic effect induced by RA compared with the MDA-MB-231 cell line. Indeed, *TNF- $\alpha$*  has been found to increase cell survival and proliferation in some cancers, including breast cancer (Szlosarek and Balkwill, 2003) through NF- $\kappa$ B activation (Luo et al., 2004). Nevertheless, the protein typically maintains tissue homeostasis by activating caspase, inhibiting the cell cycle, and inducing apoptosis (Robbs et al., 2013).

In MDA-MB-231 cells, RA upregulated the expression of two members of the proapoptotic BCL-2 family: *HRK* and *BNIP3* genes. Comparably, *BNIP3* was upregulated in MDA-MB-468 cells; however, the transcription activation of the gene was greater in MDA-MB-468 cells compared with its counterpart MDA-MB-231 cell line. The previously reported association between upregulated *TNF* and *BNIP3* upregulation (Ghavami et al., 2009) may explain the current findings.

Bcl-2 Interacting Protein (*BNIP3*) and Harakiri, a Bcl-2 Interacting Protein (*HRK*), have a C-terminal transmembrane and a motif resembling BH3 domains that are crucial for apoptosis induction (Ma et al., 2017). *BNIP3* expression is downregulated in the late stage of different types of cancer, (Erkan et al., 2005b), (Murai et al., 2005a, 2005b), and was found to correlate with chemoresistance and worse prognosis (Akada et al., 2005; Erkan et al., 2005). In BC, upregulated *BNIP3* induces apoptosis through (FAS) inhibition and inhibits cell proliferation (Bandyopadhyay et al., 2006; Khan et al., 2014) by arresting cells at the S-phase (Zhou et al., 2003). Although *BNIP3* can activate Bcl-2 and Bcl-xL, its affinity is too low to trigger cell death (Bellot et al., 2009). Additionally, the upregulation of expressed *HRK* selectively blocks the function of these anti-apoptotic proteins and induces intrinsic apoptosis by altering mitochondrial membrane permeability (Imazu et al., 1999; Inohara et al., 1997). Overexpression of *HRK* induces both intrinsic and extrinsic pathways in the prostate, ovarian, and breast cancer cells (Kaya-Aksoy et al., 2019; Lin et al., 2001).

Interestingly, in MDA-MB-468 cells, RA inhibited the expression of two proteins with different behaviors toward apoptosis: *TNFSF10* and *BIRC5* mRNAs. Based on previous reports, these inhibitions may have inconsistent effects on MDA-MB-468 cells. The smallest member of the IAP family and the highly specific tumor gene *BIRC5* (Hingorani et al., 2013) (Jha et al., 2012) suppresses apoptosis. In BC, overexpression of *BIRC5* is considered a marker in the early diagnosis of the disease, and it is correlated with the resistance to chemo and radiotherapy and poor clinical outcomes (Gunaldi et al., 2018; Jha et al., 2012).

The multifunctional *BIRC5* controls mitosis (Altieri, 2013) and prevents apoptosis by inhibiting the expression of different caspases (Shin et al., 2001), leading to metastasis and decreased survival rate. Indeed, having this gene only inhibited in MDA-MB-468, compared to MDA-MB-231 cells, strongly suggests the involvement of *BIRC5* attenuation in the higher caspase-independent apoptotic effects of RA in the MDA-MB-468 cell line.

The data indicated the dramatic suppression of *TNFRSF10* that might weaken the RA-apoptotic effect in MDA-MB-468. The gene *TNFRSF10* has the potential to induce apoptotic and autophagy, the surrogates of programmed cell death. It can activate the extrinsic apoptosis pathway once binding to its death receptors, TNFRSF10A, and TNFRSF10B (He et al., 2012; Kelley and Ashkenazi, 2004). To enhance proliferation, some cancers, however, utilize specific mechanisms such as NF- $\kappa$ B activation to control *TNFRSF10*-induced apoptosis, leading to upregulated expression of anti-apoptotic proteins (Lin et al., 2000; Wajant, 2004). Nonetheless, RA was able to have alternative mechanisms to enhance apoptosis, mediated by *BIRC5*, independent of *TNFRSF10*.

In MDA-MB-468 cells, the proapoptotic gene *GADD45A* was significantly upregulated by ~5-fold in RA-treated cells. The overexpressed *GADD45A* induces apoptosis by activating various signaling pathways, including NF- $\kappa$ B, p38 MAPK, and c-Jun amino-terminal kinase (JNK) signaling pathways (De Smaele et al., 2001; McCarthy et al., 1998; Takekawa and Saito, 1998; Zhang et al., 2010).

*GADD45A* is a member of the stress sensor family *GADD45*, which involved in many cellular functions, including DNA repair, apoptosis, cell cycle regulation, genomic stability, and immune response (Zhan, 2005). *GADD45A* can induce G<sub>1</sub> cell cycle arrest (Liebermann and Hoffman, 2007) and G<sub>2</sub>/M arrest (Wang et al., 1999). The hold on cell cycle advancement promotes apoptosis via p38 and JNK pathways (Liebermann et al., 2011). *GADD45* genes are epigenetically inactivated in different types of cancers (Al-Romaih et al., 2008). In TNBC, the low expression of the gene is strongly related to the absence of the three receptors, ER, PR, and Her2/neu (Tront et al., 2013). Consistent with previous findings (Saha et al., 2010), the upregulated expression of *GADD45A* in MDA-MB-468 could mediate the observed cell cycle arrest at the S-phase and consequential apoptosis.

In conclusion, the data presented in this study demonstrated the anticancer mechanism of the natural polyphenol compound RA in two different TNBC cell lines; MDA-MB-231 and MDA-MB-468, in which this agent altered the expression of various apoptosis-involved genes. This study found that RA was more potent against MDA-MB-468 cells in inducing mitotic arrest and apoptosis. Indeed, the data underline the importance of the compound in initiating apoptosis through extrinsic and intrinsic apoptosis-related genes. RA upregulates the proapoptotic gene *BNIP3* in both MDA-MB-231 and MDA-MB-468 cells. The RA mechanism of action on the MDA-MB-468 genotype involves extrinsic and intrinsic caspase-independent apoptosis pathways mainly. RA apoptotic effect is primarily implemented through the suppression of surviving protein *BIRC5* and the upregulation of the proapoptotic genes; *TNF*, *GADD45A*, and *BNIP3*, that could arrest the cell at its S-phase. Noticeably, the RA apoptotic mechanism in the MDA-MB-231 genotype is weaker and mainly promoted by the upregulation of *HRK*, *TNFRSF25*, and *BNIP3* as well as the

downregulation of the anti-apoptotic gene of *TNFRSF11B*. Considering the 500 mg of RA per day as a safe dose in human (Noguchi-Shinohara et al., 2015), the data obtained suggest that the polyphenol RA may have potential in TNBC therapies, particularly in MDA-MB-468 cells.

## Acknowledgments

The authors sincerely appreciate the assistance of Dr. Ramesh Badisa and the valuable editing and comments of Dr. Charles Lewis. The authors also acknowledge the biology students Mahmoud Aldawalibi and Seham Elsulami from the Dept. of Biology, Florida A&M University, for their assistance.

### Funding

The present study was supported by the United States' National Institute of Minority Health and Health Disparity through grants U54 MD007582 and P20 MD006738.

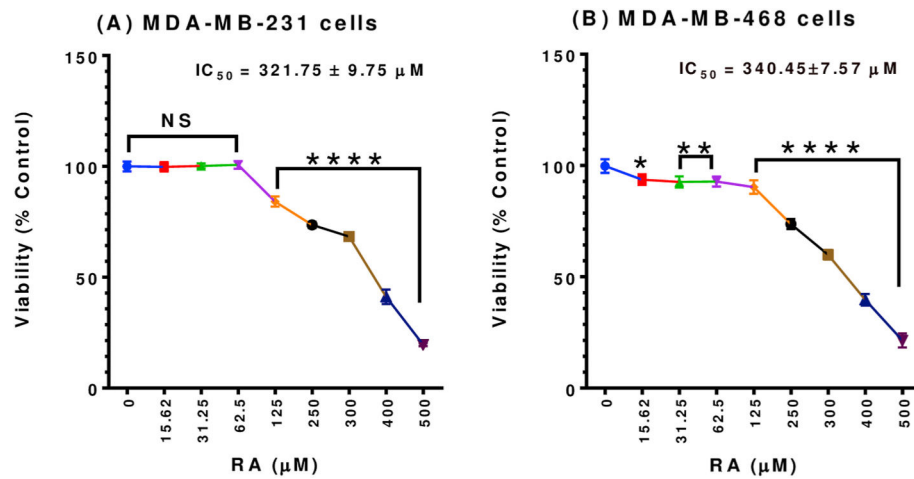
## References

- Akada M, Crnogorac-Jurcevic T, Lattimore S, Mahon P, Lopes R, Sunamura M, Matsuno S, Lemoine NR, 2005 Intrinsic chemoresistance to gemcitabine is associated with decreased expression of BNIP3 in pancreatic cancer. *Clin. Canc. Res* 11, 3094–3101.
- Al-Romaih K, Sadikovic B, Yoshimoto M, Wang Y, Zielenska M, Squire JA, 2008 Decitabine-induced demethylation of 5' CpG island in GADD45A leads to apoptosis in osteosarcoma cells. *Neoplasia* 10, 471–480. [PubMed: 18472964]
- Altieri DC, 2013 Targeting survivin in cancer. *Canc. Lett* 332, 225–228.
- Anders CK, Carey LA, 2009 Biology, metastatic patterns, and treatment of patients with triple-negative breast cancer. *Clin. Breast Canc* 9 (Suppl. 2), S73–S81.
- Bandyopadhyay S, Zhan R, Wang Y, Pai SK, Hirota S, Hosobe S, Takano Y, Saito K, Furuta E, Iizumi M, Mohinta S, Watabe M, Chalfant C, Watabe K, 2006 Mechanism of apoptosis induced by the inhibition of fatty acid synthase in breast cancer cells. *Canc. Res* 66, 5934–5940.
- Bellot G, Garcia-Medina R, Gounon P, Chiche J, Roux D, Pouyssegur J, Mazure NM, 2009 Hypoxia-induced autophagy is mediated through hypoxia-inducible factor induction of BNIP3 and BNIP3L via their BH3 domains. *Mol. Cell Biol* 29, 2570–2581. [PubMed: 19273585]
- Cao YY, Yu J, Liu TT, Yang KX, Yang LY, Chen Q, Shi F, Hao JJ, Cai Y, Wang MR, Lu WH, Zhang Y, 2018 Plumbagin inhibits the proliferation and survival of esophageal cancer cells by blocking STAT3-PLK1-AKT signaling. *Cell Death Dis.* 9, 17. [PubMed: 29339720]
- Citalingam K, Abas F, Lajis NH, Othman I, Naidu R, 2015 Antiproliferative effect and induction of apoptosis in androgen-independent human prostate cancer cells by 1,5-bis(2-hydroxyphenyl)-1,4-pentadiene-3-one. *Molecules* 20, 3406–3430. [PubMed: 25690296]
- Dai X, Ma R, Zhao X, Zhou F, 2019 Epigenetic profiles capturing breast cancer stemness for triple-negative breast cancer control. *Epigenomics* 11 (16), 1811–1825. [PubMed: 31729259]
- De Smaele E, Zazzeroni F, Papa S, Nguyen DU, Jin R, Jones J, Cong R, Franzoso G, 2001 Induction of gadd45beta by NF-kappaB downregulates proapoptotic JNK signaling. *Nature* 414, 308–313. [PubMed: 11713530]
- Erkan M, Kleeff J, Esposito I, Giese T, Ketterer K, Buchler MW, Giese NA, Friess H, 2005 Loss of BNIP3 expression is a late event in pancreatic cancer, contributing to chemoresistance and worsened prognosis. *Oncogene* 24, 4421–4432. [PubMed: 15856026]
- Fulda S, 2008 Targeting inhibitor of apoptosis proteins (IAPs) for cancer therapy. *Anti Canc. Agents Med. Chem* 8, 533–539.
- Fulda S, 2009 Tumor resistance to apoptosis. *Int. J. Canc* 124, 511–515.
- Fulda S, 2011 Targeting apoptosis signaling pathways for anticancer therapy. *Frontiers in oncology* 1, 23. [PubMed: 22655234]

- Ge Z, Sanders AJ, Ye L, Mansel RE, Jiang WG, 2013 Expression of death receptor-3 in human breast cancer and its functional effects on breast cancer cells in vitro. *Oncol. Rep* 29, 1356–1364. [PubMed: 23443464]
- Ghavami S, Eshraghi M, Kadkhoda K, Mutawe MM, Maddika S, Bay GH, Wesselborg S, Halayko AJ, Klönisch T, Los M, 2009 Role of BNIP3 in TNF-induced cell death—TNF upregulates BNIP3 expression. *Biochim. Biophys. Acta* 1793, 546–560. [PubMed: 19321129]
- Gunaldi M, Isiksacan N, Kocoglu H, Okuturlar Y, Gunaldi O, Topcu TO, Karabulut M, 2018 The value of serum survivin level in early diagnosis of cancer. *J. Canc. Res. Therapeut* 14, 570–573.
- He W, Wang Q, Xu J, Xu X, Padilla MT, Ren G, Gou X, Lin Y, 2012 Attenuation of TNFSF10/TRAIL-induced apoptosis by an autophagic survival pathway involving TRAF2- and RIPK1/RIP1-mediated MAPK8/JNK activation. *Autophagy* 8, 1811–1821. [PubMed: 23051914]
- Hingorani P, Dickman P, Garcia-Filion P, White-Collins A, Kolb EA, Azorsa DO, 2013 BIRC5 expression is a poor prognostic marker in Ewing sarcoma. *Pediatr. Blood Canc* 60, 35–40.
- Huang Y, Cai Y, Huang R, Zheng X, 2018 Rosmarinic acid combined with adriamycin induces apoptosis by triggering mitochondria-mediated signaling pathway in HepG2 and bel-7402 cells. *Med. Sci. Mon. Int. Med. J. Exp. Clin. Res.: international medical Journal of experimental and clinical research* 24, 7898–7908.
- Hudis CA, Gianni L, 2011 Triple-negative breast cancer: an unmet medical need. *Oncol.* 16 (Suppl. 1), 1–11.
- Hur YG, Yun Y, Won J, 2004 Rosmarinic acid induces p51cck-dependent apoptosis in Jurkat and peripheral T cells via the mitochondrial pathway independent from Fas/Fas ligand interaction *J. Immunol* 172, 79–87 (Baltimore, Md. : 1950). [PubMed: 14688312]
- Imazu T, Shimizu S, Tagami S, Matsushima M, Nakamura Y, Miki T, Okuyama A, Tsujimoto Y, 1999 Bcl-2/E1B 19 kDa-interacting protein 3-like protein (Bnip3L) interacts with BCL-2/Bcl-xL and induces apoptosis by altering mitochondrial membrane permeability. *Oncogene* 18, 4523–4529. [PubMed: 10467396]
- Inohara N, Ding L, Chen S, Nunez G, 1997 harakiri, a novel regulator of cell death, encodes a protein that activates apoptosis and interacts selectively with survival-promoting proteins Bcl-2 and Bcl-X(L). *EMBO J.* 16, 1686–1694. [PubMed: 9130713]
- Jan R, Chaudhry GE, 2019 Understanding apoptosis and apoptotic pathways targeted cancer therapeutics. *Adv. Pharmaceut. Bull* 9, 205–218.
- Jang YG, Hwang KA, Choi KC, 2018 Rosmarinic acid, a component of rosemary tea, induced the cell cycle arrest and apoptosis through modulation of HDAC2 expression in prostate cancer cell lines. *Nutrients* 10.
- Jha K, Shukla M, Pandey M, 2012 Survivin expression and targeting in breast cancer. *Surg Oncol* 21, 125–131. [PubMed: 21334875]
- Johnstone RW, Ruefli AA, Lowe SW, 2002 Apoptosis: a link between cancer genetics and chemotherapy. *Cell* 108, 153–164. [PubMed: 11832206]
- Katsman A, Umezawa K, Bonavida B, 2009 Chemosensitization and immunosensitization of resistant cancer cells to apoptosis and inhibition of metastasis by the specific NF-kappaB inhibitor DHMEQ. *Curr. Pharmaceut. Des* 15, 792–808.
- Kaya-Aksoy E, Cingoz A, Senbabaoglu F, Seker F, Sur-Erdem I, Kayabolen A, Lokumcu T, Sahin GN, Karahuseyinoglu S, Bagci-Onder T, 2019 The proapoptotic Bcl-2 family member Harakiri (HRK) induces cell death in glioblastoma multiforme. *Cell death discovery* 5, 64. [PubMed: 30774992]
- Kelley SK, Ashkenazi A, 2004 Targeting death receptors in cancer with Apo2L/TRAIL. *Curr. Opin. Pharmacol* 4, 333–339. [PubMed: 15251125]
- Khan A, Aljarbou AN, Aldebasi YH, Faisal SM, Khan MA, 2014 Resveratrol suppresses the proliferation of breast cancer cells by inhibiting fatty acid synthase signaling pathway. *Cancer Epidemiology* 38, 765–772. [PubMed: 25448084]
- Kuo PL, Hsu YL, Cho CY, 2006 Plumbagin induces G2-M arrest and autophagy by inhibiting the AKT/mammalian target of rapamycin pathway in breast cancer cells. *Mol. Canc. Therapeut* 5, 3209–3221.
- LaCasse EC, Mahoney DJ, Cheung HH, Plenchette S, Baird S, Korneluk RG, 2008 IAP-targeted therapies for cancer. *Oncogene* 27, 6252–6275. [PubMed: 18931692]

- Li H, Zhuang HL, Lin JJ, Zhang YF, Huang H, Luo T, Yu WT, Ni F, 2018 Effect of rosmarinic acid from *Sarcandra glabra* in inhibiting proliferation and migration and inducing apoptosis of MDA-MB-231 cells via regulation of expressions of Bcl-2 and Bax]. *Zhongguo Zhong Yao za Zhi = Zhongguo Zhong Yao za Zhi = China Journal of Chinese materia medica* 43, 3335–3340. [PubMed: 30200738]
- Liebermann DA, Hoffman B, 2007 Gadd45 in the response of hematopoietic cells to genotoxic stress. *Blood Cell Mol. Dis* 39, 329–335.
- Liebermann DA, Tront JS, Sha X, Mukherjee K, Mohamed-Hadley A, Hoffman B, 2011 Gadd45 stress sensors in malignancy and leukemia. *Crit. Rev. Oncog* 16, 129–140. [PubMed: 22150313]
- Lin J, Page C, Jin X, Sethi AO, Patel R, Nunez G, 2001 Suppression activity of proapoptotic gene products in cancer cells, a potential application for cancer gene therapy. *Anticancer Res.* 21, 831–839. [PubMed: 11396172]
- Lin Y, Devin A, Cook A, Keane MM, Kelliher M, Lipkowitz S, Liu ZG, 2000 The death domain kinase RIP is essential for TRAIL (Apo2L)-induced activation of IkappaB kinase and c-Jun N-terminal kinase. *Mol. Cell Biol* 20, 6638–6645. [PubMed: 10958661]
- Luo JL, Maeda S, Hsu LC, Yagita H, Karin M, 2004 Inhibition of NF-kappaB in cancer cells converts inflammation-induced tumor growth mediated by TNFalpha to TRAIL-mediated tumor regression. *Canc. Cell* 6, 297–305.
- Ma Z, Chen C, Tang P, Zhang H, Yue J, Yu Z, 2017 BNIP3 induces apoptosis and protective autophagy under hypoxia in esophageal squamous cell carcinoma cell lines: BNIP3 regulates cell death. *Dis. Esophagus: official Journal of the International Society for Diseases of the Esophagus* 30, 1–8.
- McCarthy JV, Ni J, Dixit VM, 1998 RIP2 is a novel NF-kappaB-activating and cell death-inducing kinase. *J. Biol. Chem* 273, 16968–16975. [PubMed: 9642260]
- Messeha SS, Zarmouh NO, Mendonca P, Alwagdani H, Cotton C, Soliman KFA, 2019 Effects of gossypol on apoptosis-related gene expression in racially distinct triple-negative breast cancer cells. *Oncol. Rep* 42, 467–478. [PubMed: 31173249]
- Murai M, Toyota M, Satoh A, Suzuki H, Akino K, Mita H, Sasaki Y, Ishida T, Shen L, Garcia-Manero G, Issa JP, Hinoda Y, Tokino T, Imai K, 2005a Aberrant DNA methylation associated with silencing BNIP3 gene expression in haematopoietic tumours. *Br. J. Canc* 92, 1165–1172.
- Murai M, Toyota M, Suzuki H, Satoh A, Sasaki Y, Akino K, Ueno M, Takahashi F, Kusano M, Mita H, Yanagihara K, Endo T, Hinoda Y, Tokino T, Imai K, 2005b Aberrant methylation and silencing of the BNIP3 gene in colorectal and gastric cancer. *Clin. Canc. Res* 11, 1021–1027.
- Noguchi-Shinohara M, Ono K, Hamaguchi T, Iwasa K, Nagai T, Kobayashi S, Nakamura H, Yamada M, 2015 Pharmacokinetics, safety, and tolerability of melissa officinalis extract which contained rosmarinic acid in healthy individuals: a randomized controlled trial. *PLoS One* 10 e0126422. [PubMed: 25978046]
- Plati J, Bucur O, Khosravi-Far R, 2008 Dysregulation of apoptotic signaling in cancer: molecular mechanisms and therapeutic opportunities. *J. Cell. Biochem* 104, 1124–1149. [PubMed: 18459149]
- Rahman KW, Li Y, Wang Z, Sarkar SH, Sarkar FH, 2006 Gene expression profiling revealed survivin as a target of 3,3'-diindolylmethane-induced cell growth inhibition and apoptosis in breast cancer cells. *Canc. Res* 66, 4952–4960.
- Ramachandran C, Rodriguez S, Ramachandran R, Raveendran Nair PK, Fonseca H, Khatib Z, Escalon E, Melnick SJ, 2005 Expression profiles of apoptotic genes induced by curcumin in human breast cancer and mammary epithelial cell lines. *Anticancer Res.* 25, 3293–3302. [PubMed: 16101141]
- Rath PC, Aggarwal BB, 1999 TNF-induced signaling in apoptosis. *J. Clin. Immunol* 19, 350–364. [PubMed: 10634209]
- Robbs BK, Lucena PI, Viola JP, 2013 The transcription factor NFAT1 induces apoptosis through cooperation with Ras/Raf/MEK/ERK pathway and upregulation of TNF-alpha expression. *Biochim. Biophys. Acta* 1833, 2016–2028. [PubMed: 23583303]
- Ryu H, Nam KY, Kim JS, Hwang SG, Song JY, Ahn J, 2018 The small molecule AU14022 promotes colorectal cancer cell death via p53-mediated G2/M-phase arrest and mitochondria-mediated apoptosis. *J. Cell. Physiol* 233, 4666–4676. [PubMed: 29030986]

- Sadighi S, Zokaasadi M, Kasaeian A, Maghsudi S, Jahanzad I, Kamranzadeh Fumani H, 2017 The effect of immunohistochemically detected p53 accumulation in the prognosis of breast cancer; A retrospective survey of the outcome. *PloS One* 12, e0182444. [PubMed: 28771563]
- Saha A, Kuzuhara T, Echigo N, Fujii A, Suganuma M, Fujiki H, 2010 Apoptosis of human lung cancer cells by curcumin mediated through up-regulation of “growth arrest and DNA damage-inducible genes 45 and 153. *Biol. Pharm. Bull* 33, 1291–1299. [PubMed: 20686221]
- Sato N, Beitz JG, Kato J, Yamamoto M, Clark JW, Calabresi P, Raymond A, Frackelton AR Jr., 1993 Platelet-derived growth factor indirectly stimulates angiogenesis in vitro. *Am. J. Pathol* 142, 1119–1130. [PubMed: 7682762]
- Shin S, Sung BJ, Cho YS, Kim HJ, Ha NC, Hwang JI, Chung CW, Jung YK, Oh BH, 2001 An anti-apoptotic protein human survivin is a direct inhibitor of caspase-3 and -7. *Biochemistry* 40, 1117–1123. [PubMed: 11170436]
- Silva JC, Ferreira-Strixino J, Fontana LC, Paula LM, Raniero L, Martin AA, Canevari RA, 2014 Apoptosis-associated genes related to photodynamic therapy in breast carcinomas. *Laser Med. Sci* 29, 1429–1436.
- Szlosarek PW, Balkwill FR, 2003 Tumour necrosis factor alpha: a potential target for the therapy of solid tumours. *Lancet Oncol.* 4, 565–573. [PubMed: 12965278]
- Takekawa M, Saito H, 1998 A family of stress-inducible GADD45-like proteins mediate activation of the stress-responsive MTK1/MEKK4 MAPKKK. *Cell* 95, 521–530. [PubMed: 9827804]
- Teoh PL, Liao M, Cheong BE, 2019 *Phyllanthus nodiflora* L. Extracts induce apoptosis and cell cycle arrest in human breast cancer cell line, MCF-7. *Nutr. Canc* 71, 668–675.
- Tront JS, Willis A, Huang Y, Hoffman B, Liebermann DA, 2013 Gadd45a levels in human breast cancer are hormone receptor-dependent. *J. Transl. Med* 11, 131. [PubMed: 23706118]
- Wajant H, 2004 TRAIL and NFkappaB signaling—a complex relationship. *Vitam. Horm* 67, 101–132. [PubMed: 15110174]
- Wang XW, Zhan Q, Coursen JD, Khan MA, Kontny HU, Yu L, Hollander MC, O’Connor PM, Fornace AJ Jr., Harris CC, 1999 GADD45 induction of a G2/M cell cycle checkpoint. *Proc. Natl. Acad. Sci. U. S. A* 96, 3706–3711. [PubMed: 10097101]
- Yamamoto H, Omelchenko I, Shi X, Nuttall AL, 2009 The influence of NF-kappaB signal-transduction pathways on the murine inner ear by acoustic overstimulation. *J. Neurosci. Res* 87, 1832–1840. [PubMed: 19185019]
- Yesil-Celiktas O, Sevimli C, Bedir E, Vardar-Sukan F, 2010 Inhibitory effects of rosemary extracts, carnosic acid, and rosmarinic acid on the growth of various human cancer cell lines. *Plant Foods Hum. Nutr. (Dordr.)* 65, 158–163.
- Zhan Q, 2005 Gadd45a, a p53- and BRCA1-regulated stress protein, in the cellular response to DNA damage. *Mutat. Res* 569, 133–143. [PubMed: 15603758]
- Zhang D, Lin J, Han J, 2010 Receptor-interacting protein (RIP) kinase family. *Cell. Mol. Immunol* 7, 243–249. [PubMed: 20383176]
- Zhang HW, Hu JJ, Fu RQ, Liu X, Zhang YH, Li J, Liu L, Li YN, Deng Q, Luo QS, Ouyang Q, Gao N, 2018 Flavonoids inhibit cell proliferation and induce apoptosis and autophagy through downregulation of PI3Kgamma mediated PI3K/AKT/mTOR/p70S6K/ULK signaling pathway in human breast cancer cells. *Sci. Rep* 8, 11255. [PubMed: 30050147]
- Zhou W, Simpson PJ, McFadden JM, Townsend CA, Medghalchi SM, Vadlamudi A, Pinn ML, Ronnett GV, Kuhajda FP, 2003 Fatty acid synthase inhibition triggers apoptosis during the S phase in human cancer cells. *Canc. Res* 63, 7330–7337.

**Fig. 1.**

Effect of RA on the viability of (A) MDA-MB-231 and (B) MDA-MB-468 TNBC cell lines. Both cell lines were plated and treated similarly for 48 h with RA at concentration ranges of 0–500  $\mu M$ . The graph shows the cell viability data expressed as percentages of cell survival compared to the control. The data points represent the mean  $\pm$  S.E.M. of two independent studies,  $n = 5$  each. One-way analysis of variance (ANOVA) followed by Bonferroni's multiple comparisons test was used to determine the significance of the difference between the control and treated groups. The difference was considered significant at \* $P < 0.05$ , \*\* $P < 0.01$ , and \*\*\*\* $P < 0.0001$ . NS, non-significant.

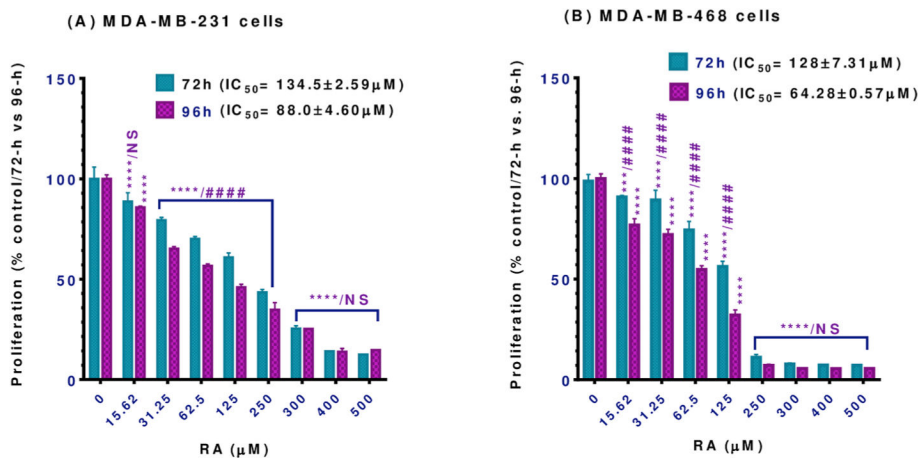


**Fig. 2.** Effect of RA on proliferation in (A) MDA-MB-231 and (B) MDA-MB-468 TNBC cell lines. Both cell lines were incubated for 72 and 96 h with RA at concentration ranges of 0–500 μM. Each data point represents the mean ± S.E.M. of two independent experiments, n = 5 each. One-way ANOVA tests were used to calculate P-values for the difference between control vs. 72 or 96h exposure (\*) and two-way ANOVA tests were used to calculate P-values for the difference between the different exposure periods (#). Both one-way and two-way ANOVA analyses were followed by Bonferroni’s multiple comparisons test. \*\*\*P < 0.001 and \*\*\*\*\*/#####P < 0.0001 indicate a statistically significant difference between control vs. different exposure periods or between 72 vs. 96h exposure periods. NS, non-significant.

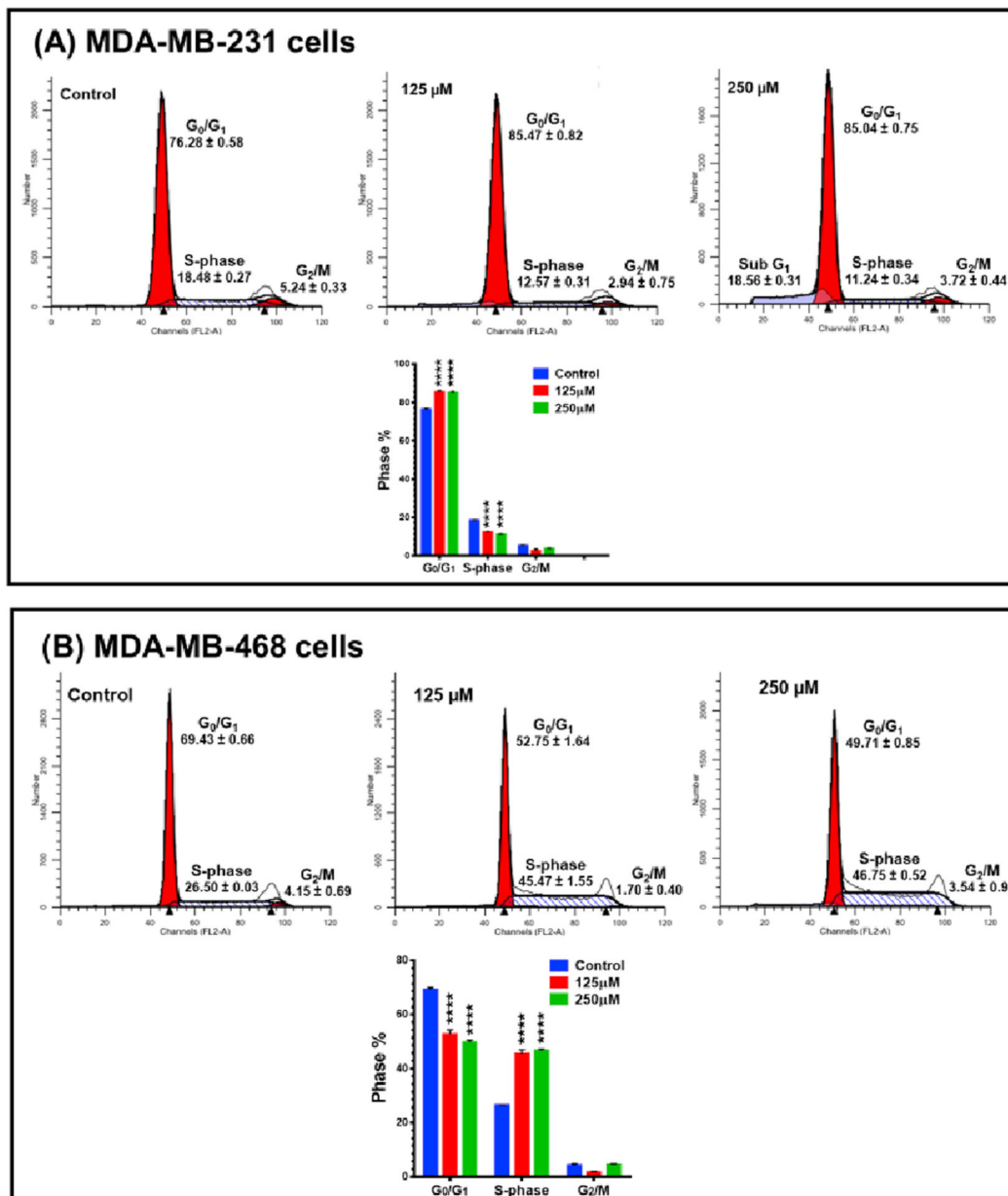


**Fig. 3.** Effect of RA on cell cycle distribution in (A) MDA-MB-231 and (B) MDA-MB-468 TNBC cell lines. Both cell lines were incubated for 48 h with RA at two concentration levels, 125 and 250 μM. Flow cytometry analysis of cell distribution is shown by PI fluorescence histograms. The experiment was repeated three times. RA induced G<sub>0</sub>/G<sub>1</sub> cell cycle arrest in MDA-MB-231 cells and S-phase arrest in MDA-MB-468 cells. One-way ANOVA, followed by Bonferroni’s multiple comparisons tests were used to determine P -values for the difference between the control and different phases of the cell cycle. The difference was considered significant at \*\*\*\*P < 0.0001.

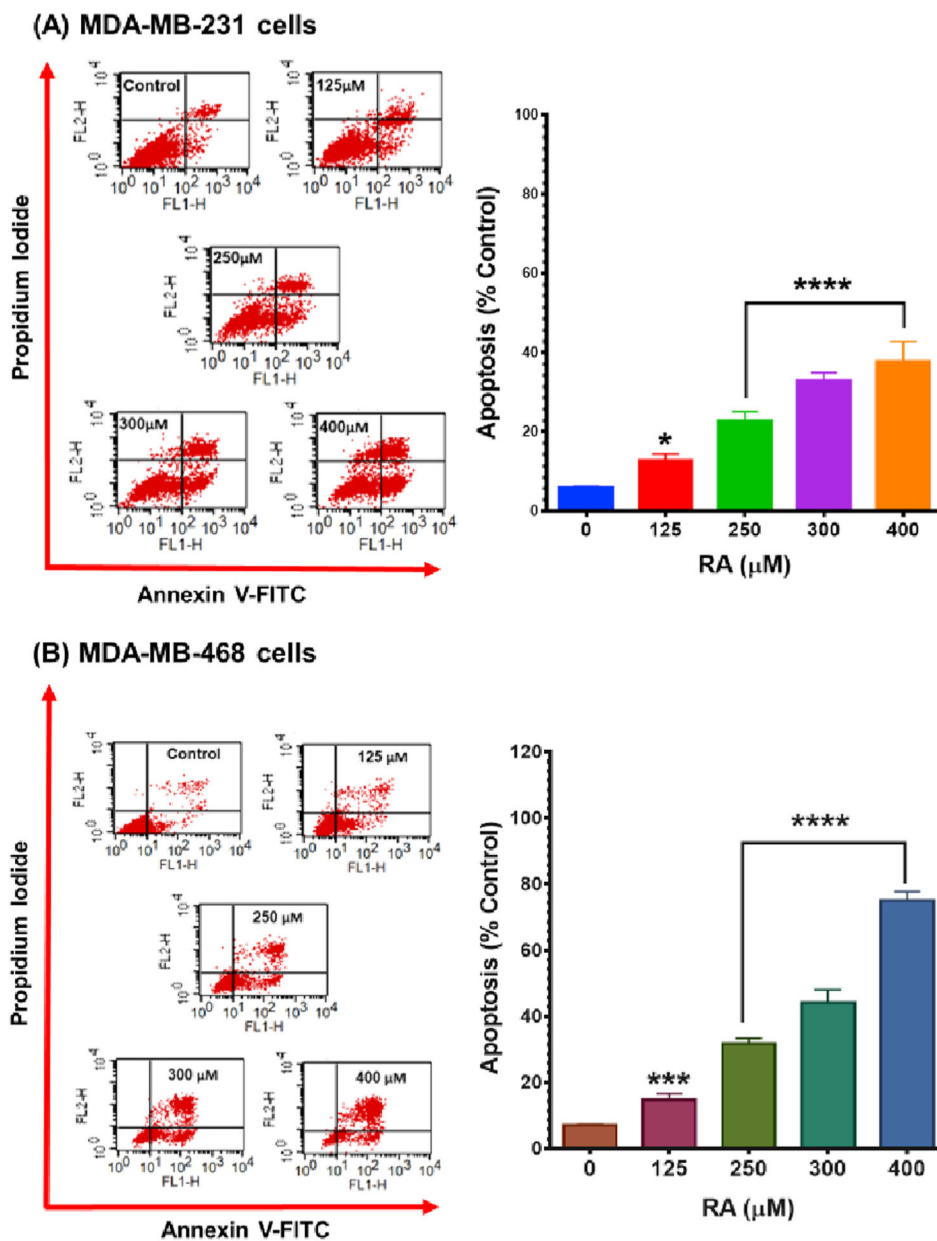


**Fig. 4.** Apoptotic effect of RA in (A) MDA-MB-231 and (B) MDA-MB-468 TNBC cell lines. Both cell lines were exposed to RA for 48 h at concentrations ranging from 0 to 400 μM. Control cells were exposed only to experimental media. An Annexin V-FITC apoptosis kit was used to label treated/control cells, and a FACSCalibur flow cytometer was used to analyze the percentage of apoptotic cells in RA-treated samples as well as the control. Each data point in the bar graphs represents the mean ± S.E.M. of two independent studies, n = 3 each. The significance of the difference between control and each treatment was calculated using one-way ANOVA followed by Bonferroni's multiple comparisons test. \*P < 0.05, \*\*\*P < 0.001, and \*\*\*\*P < 0.0001 indicated the statistically significant difference.

## Apoptosis Array (SAB Target List) H 96, Human

### (A) MDA-MB-231 cells

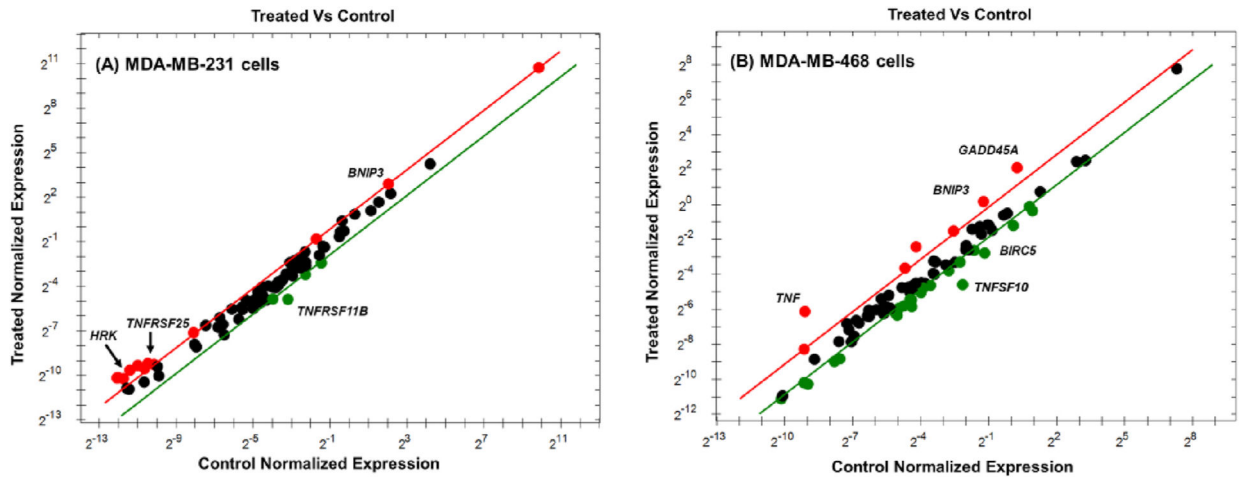
	1	2	3	4	5	6	7	8	9	10	11	12	
A	ABL1	BAO3	BCL2L11	BIRC5	CASP2	CD27	CYC3	GUSB	NFAB1	TNFRSF10B	TNFRSF8	TSP	A
B	ACTB	BAK1	BCL2L2	BNIP2	CASP3	CD40	DAPK1	HRK	NOD1	TNFRSF11B	TP53	GAPDH	B
C	AIFM1	BAX	BFAR	BNIP3	CASP4	CD40LG	DFFA	IGF1R	NOL3	TNFRSF1A	TP53BP2	HRPT1	C
D	ARK1	BCL10	BID	BNIP3L	CASP5	CD70	DIABLO	IL10	PTCARD	TNFRSF1B	TPP3	GONA	D
E	ARAF1	BCL2	BIK	BRAF	CASP6	CFLAR	FADD	LVA	RIPK2	TNFRSF21	TRADD	PCR	E
F	B2M	BCL2A1	BIRC2	CASP1	CASP7	CIDEA	FAS	LYER	RPLP0	TNFRSF25	TRAF2	RO1	F
G	BAD	BCL2L1	BIRC3	CASP10	CASP8	CIDEB	FASLG	MCL1	TNF	TNFRSF9	TRAF3	RO2	G
H	BAO1	BCL2L10	BIRC5	CASP14	CASP9	CRADD	GADD45A	NAP	TNFRSF10A	TNFRSF10	XIAP	RT	H
	1	2	3	4	5	6	7	8	9	10	11	12	

### (B) MDA-MB-468 cells

	1	2	3	4	5	6	7	8	9	10	11	12	
A	ABL1	BAO3	BCL2L11	BIRC5	CASP2	CD27	CYC3	GUSB	NFAB1	TNFRSF10B	TNFRSF8	TSP	A
B	ACTB	BAK1	BCL2L2	BNIP2	CASP3	CD40	DAPK1	HRK	NOD1	TNFRSF11B	TP53	GAPDH	B
C	AIFM1	BAX	BFAR	BNIP3	CASP4	CD40LG	DFFA	IGF1R	NOL3	TNFRSF1A	TP53BP2	HRPT1	C
D	ARK1	BCL10	BID	BNIP3L	CASP5	CD70	DIABLO	IL10	PTCARD	TNFRSF1B	TPP3	GONA	D
E	ARAF1	BCL2	BIK	BRAF	CASP6	CFLAR	FADD	LVA	RIPK2	TNFRSF21	TRADD	PCR	E
F	B2M	BCL2A1	BIRC2	CASP1	CASP7	CIDEA	FAS	LYER	RPLP0	TNFRSF25	TRAF2	RO1	F
G	BAD	BCL2L1	BIRC3	CASP10	CASP8	CIDEB	FASLG	MCL1	TNF	TNFRSF9	TRAF3	RO2	G
H	BAO1	BCL2L10	BIRC5	CASP14	CASP9	CRADD	GADD45A	NAP	TNFRSF10A	TNFRSF10	XIAP	RT	H
	1	2	3	4	5	6	7	8	9	10	11	12	

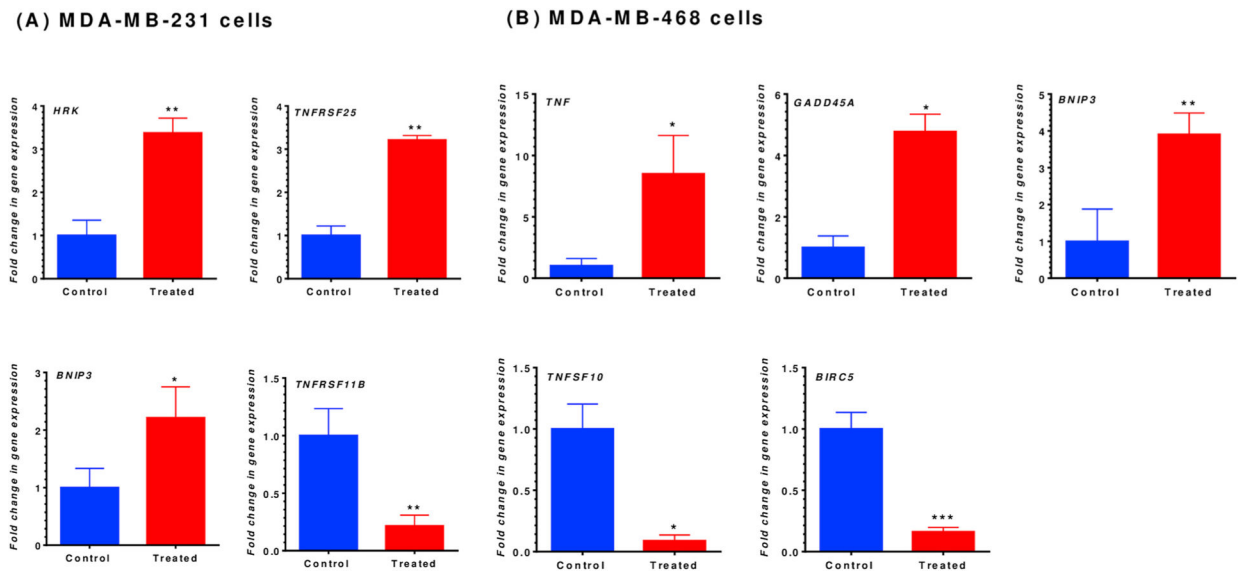
**Fig. 5.**

Effect of RA on mRNA gene expression in (A) MDA-MB-231 and (B) MDA-MB-468 TNBC cell lines using qRT-PCR. Human apoptosis array was used to measure the transcription activation in various apoptosis-involved genes. In MDA-MB-231 cells (A), the upregulated genes, HRK, TNFRSF25, and BNIP3 are framed with red color, while the downregulated gene, TNFRSF11B, is presented with a green square. Similarly, in MDA-MB-468 cells (B), the upregulated TNF, BNIP3, and GADD45A are bordered by red, and the repressed TNFSF10 and BIRC5 are shown with green-colored frames. HRK, harakiri; TNFRSF25, tumor necrosis factor receptor superfamily 25; BNIP3, BCL2 interacting protein 3; TNFRSF11B, tumor necrosis factor receptor superfamily 11B; TNF, tumor necrosis factor; BIRC5, baculoviral IAP repeat-containing 5; GADD45A, the growth arrest and DNA damage-inducible 45 alpha; TNFSF10, ligand tumor necrosis factor superfamily member 10.



**Fig. 6.**

Scatter plot for MDA-MB-231 (A) and MDA-MB-468 (B) TNBC cells. Both cell lines were exposed to RA for 48 h at a concentration of 350  $\mu\text{M}$ . The mRNA expression of target genes for the control vs. treated cells was normalized. Based on the threshold set, the plot images show the changes in various apoptosis-related gene expression as follows: upregulation, red dots, downregulation, green dots, and no changes, black dots.

**Fig. 7.**

Gene expression quantification for MDA-MB-231 (A) and MDA-MB-468 (B) TNBC cells. Both cell lines were exposed to RA for 48-h at a concentration of 350  $\mu$ M. Normalized mRNA expression data for the control vs. treated cells showed a significant impact on gene expression in both cell lines. In MDA-MB-231 cells, RA upregulated three genes (HRK, TNFRSF25, and BNIP3), while TNFRSF11B was significantly inhibited. Similarly, in MDA-MB-468 cells, three genes were significantly upregulated, including TNF, GADD45A, and BNIP3, while TNFSF10 and BIRC5 were repressed. The data points represented the mean  $\pm$  S.E.M. of at least four independent experiments. The significance of the difference was determined using an unpaired t-test between the control vs. treated cells. The difference was considered significant at \* $P < 0.05$ , \*\* $P < 0.01$ , and \*\*\* $P < 0.001$ . RA, rosmarinic acid; MDA-MB-231, MDA-MB-231; HRK, harakiri; TNFRSF25, tumor necrosis factor receptor superfamily 25; BNIP3, BCL2 interacting protein 3; TNFRSF11B, tumor necrosis factor receptor superfamily 11B; TNF, tumor necrosis factor; BIRC5, baculoviral IAP repeat-containing 5; GADD45A, the growth arrest, and DNA damage-inducible 45 alpha; TNFSF10, ligand tumor necrosis factor superfamily member 10.

**Table 1**

mRNA gene expression fold changes in MM-231 and MM-468 TNBC cells after exposure to RA for 48 h. In MM-231 cells (left panel), *HRK*, *TNFRSF25*, and *BNIP3* were upregulated, while *TNFRSF11B* was repressed. Comparably, MM-468 cells (right panel) *TNF*, *GADD45A* and *BNIP3*, were upregulated, while *TNFSF10* and *BIRC5* were inhibited.

Control vs. treated MM-231 cells			Control vs. treated MM-468 cells		
Target gene	Fold changes	p-value	Target gene	Fold changes	p-value
<i>HRK</i>	+3.38	0.0011	<i>TNF</i>	+8.50	0.0496
<i>TNFRSF25</i>	+3.21	0.0060	<i>GADD45A</i>	+4.78	0.0496
<i>BNIP3</i>	+2.21	0.0295	<i>BNIP3</i>	+3.91	0.0087
<i>TNFRSF11B</i>	- 4.65	0.0057	<i>TNFSF10</i>	- 11.25	0.0496
			<i>BIRC5</i>	- 6.19	0.0005